Tropical Biomedicine 41(1): 84-96 (2024)
https://doi.org/10.47665/tb.41.1.011

RESEARCH ARTICLE

Construction of multi-epitope vaccine against the *Rhipicephalus microplus* tick: an immunoinformatics approach

Younas, M.[1], Ashraf, K.[1], Ijaz, M.[2], Suleman, M.[3], Chohan, T.A.[4*], Rahman, S.U.[1], Rashid, M.I.[1*]

[1]Department of Parasitology, University of Veterinary and Animal Sciences, Lahore, Pakistan
[2]Department of Veterinary Medicine, University of Veterinary and Animal Sciences, Lahore 54200, Pakistan
[3]Institute of Microbiology, University of Veterinary and Animal Sciences, Lahore 54200, Pakistan
[4]Institute of Pharmaceutical Sciences, University of Veterinary and Animal Sciences, Lahore 54200, Pakistan
*Corresponding authors: imran.rashid@uvas.edu.pk; tahir.chohan@uvas.edu.pk

ARTICLE HISTORY

Received: 24 May 2023
Revised: 6 November 2023
Accepted: 7 November 2023
Published: 25 March 2024

ABSTRACT

Rhipicephalus microplus, known as the hard tick, is a vector for the parasites *Babesia* spp. and *Anaplasma marginale*, both of which can cause significant financial losses to the livestock industry. There is currently no effective vaccine for *R. microplus* tick infestations, despite the identification of numerous prospective tick vaccine candidates. As a result, the current research set out to develop an immunoinformatics-based strategy using existing methods for designing a multi-epitope based vaccination that is not only effective but also safe and capable of eliciting cellular and humoral immune responses. First, *R. microplus* proteins Bm86, Subolesin, and Bm95 were used to anticipate and link B and T-cell epitopes (HTL and CTL) to one another. Antigenicity testing, allergenicity assessment, and toxicity screening were just a few of the many immunoinformatics techniques used to identify potent epitopes. Multi-epitope vaccine design was chosen based on the antigenic score 0.935 that is promising vaccine candidate. Molecular docking was used to determine the nature of the interaction between TLR2 and the vaccine construct. Finally, molecular dynamic simulation was used to assess the stability and compactness of the resulting vaccination based on docking scores. The developed vaccine was shown to be stable, have immunogenic qualities, be soluble, and to have high expression by *in silico* cloning. These findings suggest that experimental investigation of the multi-epitope based vaccine designed in the current study will produce achievable vaccine candidates against *R. microplus* ticks, enabling more effective control of infestations.

Keywords: *Rhipicephalus microplus*; immunoinformatic tools; multi-epitope vaccine; molecular docking; molecular dynamic simulations.

INTRODUCTION

Ticks are blood-feeding parasites that parasitize vertebrate hosts all over the world. *Rhipicephalus microplus* is the most prominent tick species that is widely dispersed in cattle throughout the world (Barker & Murrell, 2004; Estrada-Peña *et al*., 2006). It declines cattle milk and meat production directly, and it indirectly transmits diseases such as Anaplasmosis and Babesiosis, both of which have detrimental impacts on cattle health and production (Peter *et al*., 2005). Both diseases cause large annual output losses in the animal business. Tick control is difficult due to its few enemies; hence integrated tick management strategies have been adopted. Chemical acaricides are used in integrated tick control programs. Acaricides can cause acaricide-resistant ticks, residues of drugs in the environment, and tainted meat and milk (Graf *et al*., 2004). Immunological control is an alternative strategy that has been adapted to control and prevent tick infestations. Vaccination is the preferred method since it has the highest probability of success, lowest cost, longest lifespan, and least impact on the environment (De la Fuente & Kocan, 2006; Sonenshine *et al*., 2006; Willadsen, 2006). In 1990, a recombinant tick vaccination targeting *R. microplus's* Bm86 gut-antigen was developed and commercialized (Rand *et al*., 1989; Willadsen *et al*., 1989; Rodríguez *et al*., 1994; Willadsen, 2006). These vaccines contained the potency to protect and trigger the immune response (Rand *et al*., 1989) and were registered and commercialized in Australia (TickGARD) and Latin American countries (Gavac) during 1993-1997 (de la Fuente *et al*., 2007). Tick populations can be reduced with the use of the Bm86 gut-antigen vaccination by decreasing the number of engorging female ticks, their egg mass and production, and their reproductive effectiveness. The results of applying the integrated tick management technique demonstrated the approach's benefits, which include being cost-effective, environmentally friendly, and preventing the development of resistant ticks. In addition to reducing the tick population, this strategy also directly reduces the spread of numerous diseases (De La Fuente *et al*., 1998; Valle *et al*., 2004; de la Fuente *et al*., 2007). In randomized controlled studies of vaccinations, it was found that the Bm86 vaccine containing *R.*

microplus provided cross-protection against various ticks, including *R. annulatus* and *R. decoloratus* (Fragoso *et al*., 1998; Dela Fuente *et al*., 2000; De Vos *et al*., 2001). The presence of Bm86 amino acid sequence variations due to genetic diversity may affect the efficacy of the vaccine in various regions of the world (García-García *et al*., 1999; Freeman *et al*., 2010). Thus, a multi-epitope-based tick vaccination could provide specific protection and improve efficacy. Antigenic variations enable discovering, screening, and validating prospective antigens for multi-epitope vaccine design challenging (Shaffer *et al*., 2016). The multi-epitope vaccination strategy can produce long-lasting protection with minimal side effects (Zhang *et al*., 2018). For the first time, it has been shown that tick vaccines can be designed using epitopes (Patarroyo *et al*., 2002; Gershoni *et al*., 2007; Childs *et al*., 2015; Ahmad *et al*., 2016). Thus, shifting from an antigen-based vaccine to an epitope-based vaccine may improve the effectiveness of the tick vaccine. Recent advances in computational approaches have allowed for the successful design of multi-epitope-based vaccinations, adjuvants, and antibodies employing a wide variety of immune-informatics tools (Patarroyo *et al*., 2002; Mehla & Ramana, 2016; Gaafar *et al*., 2019). Therefore, these bioinformatics tools helped in the developed of a multi-epitope vaccination that shows promise as a preventative measure. Here, we developed a vaccine that targets many epitopes using immunoinformatic techniques. *Rhipicephalus microplus* proteins Bm86, subolesin, and Bm95 were employed. Each of these three proteins is crucial in eliciting a protective immune response against ticks (Younas *et al*., 2023a). This vaccine incorporated epitopes from all three types of helper T lymphocytes (HTL), cytotoxic T lymphocytes (CTL), and B lymphocytes. The humoral and cellular response of the immune system may be strengthened by this vaccination, increasing its efficacy against *R. microplus* ticks. Through molecular docking and molecular dynamic simulation, we were able to analyse the vaccine construct's interaction with Toll Like Receptor-2 (TLR-2) and its stability, as well as its immunogenicity, allergenicity, and physicochemical properties. *In-silico* cloning was done by SnapGene software to further assess the construct's capability of producing proteins with high levels of expression and translation efficiency. This proposed multi-epitope-based vaccination design needs to be tested in a controlled environment before it can be utilized to control *R. microplus* tick populations.

MATERIALS AND METHODS

Rhipicephalus microplus antigenic proteins

The three proteins of *R. microplus* (Bm86, subolesin, and Bm95) were selected after the comprehensive study of literature and their sequences were retrieved from national center for biotechnology information (NCBI) in FASTA format. The scratch protein predictor server was used to predict the antigenicity of proteins (https://scratch.proteomics.ics.uci.edu/)(Magnan *et al*., 2010).

Identification of Helper T-Lymphocyte epitopes

Immune Epitope and Analysis Resource (IEDB) server (http://tools.iedb.org/mhcii/) was employed for the identification of Helper T-cell epitopes (15-mers in length) of three target proteins. The reference allele MHC class II HLA allele was chosen because it accounts for 99.9% of the allele distribution. It predicts HTL epitopes based on percentile rank and low IC50 values while keeping all other parameters at their default values. HTL epitopes were identified by choosing the HLA Class II DRB I allele, a low percentile rank, and IC50 values. Epitopes with significant binding affinity to MHC II receptors were predicted (Lin *et al*., 2008).

Identification of Interferon-γ (IFN-γ) epitope

Interferon-γ was predicted through an IFN-γ server in which HTL epitopes were used as input and it categorizes the epitopes as either negative or positive inducers by using a support vector machine (SVM) approach (http://crdd.osdd.net/raghava/ifnepitope/). The SVM and Motif method was selected and the cytokine versus IFN model was chosen. The IFN-γ server has a dataset of 6728 non-inducing and 3705-inducing binders from IEDB (Dhanda *et al*., 2013).

Cytotoxic T-Lymphocyte epitope identification

NetCTL 1.2 server was used to predict the CTL epitopes recognized by MHC-class I supertypes A2, A3, and B7 (Larsen *et al*., 2007). The epitopes were predicted to keep the default values of weight on TAP transport efficiency, C-terminal cleavage, and MHC class-I binding affinity. The predicted CTL epitopes were further perused for immunogenicity evaluation using IEDB class I immunogenicity (Calis *et al*., 2013). The epitopes with higher scores were considered potential epitopes with strong binding affinity and were used for vaccine designing.

Prediction of B-cell epitopes

The B-cell epitopes play a significant role in enhancing the immune response by being recognized by the receptor of B-lymphocyte. The B-cell epitopes were predicted by ABCpred server (Malik *et al*., 2021). This server predicts the epitopes using an artificial neural network. The ABCpred server contains epitopes of various organisms such as parasites, bacteria, and viruses with 65.9% accuracy.

Toxicity prediction

The predicted epitopes were further evaluated for toxicity prediction using the ToxinPred server (Gupta *et al*., 2013). After being confirmed to be non-toxic, the proposed epitopes were used in vaccine design.

Construction of a multi-epitope vaccine

Finally, a multi-epitope-based construct was developed using previously reported approaches, including the use of selected HTL, CTL, and B-cell epitopes (Yadav *et al*., 2020). Suitable linkers were added to give amino acids flexibility; they were required to fold into desirable conformations. An adjuvant 50S ribosomal protein L7/L12 is added to enhance immunity and increase the effectiveness of the vaccine upon immunization in vaccinated calves. This adjuvant can act as an agonist for Toll-like receptor (TLR) and could induce the antigen-specific immune response upon immunization (Marciani, 2003; Khatoon *et al*., 2017) We used the 50S ribosomal L7/L12 UniProt database's (P9WHE3) 130-amino-acid long, which was connected to the N-terminus as adjuvant using linker EAAAK. Adjuvants improve efficacy by increasing immunogenicity. GPGPG linkers were employed to connect HTL epitopes, KK linkers to B-cell, and AAY linkers to connect CTL epitopes (Pandey *et al*., 2018; Kalita *et al*., 2020a).

Predicting physicochemical properties, immunogenicity, and allergenicity

The antigenicity and immunogenicity of the designed vaccine were determined using ANTIGENPro (Magnan *et al*., 2010) and VaxiJen 2.0 server (Doytchinova & Flower, 2007) respectively. It predicts antigenicity based on autonomous alignment. Immunogenicity refers to a vaccine's ability to prime the immune system to respond strongly to both outside invaders and additional vaccines. The allergenicity of constructed vaccine was evaluated by AllerTOP v2.0 (Dimitrov *et al*., 2014). The multi-epitope-based-designed construct physicochemical properties were assessed by the ExPASY Protparam server (Gasteiger *et al*., 2005).

Prediction of secondary and tertiary structures and validation of the designed construct

The vaccine construct's secondary and tertiary structures were determined with the PSIPred online tool and the RaptorX server, respectively (McGuffin *et al*., 2000; Källberg *et al*., 2014). The RaptorX software was used to evaluate the tertiary structure of the proposed vaccine by inputting its amino acid sequence into

it. The 3D structure prediction was verified and refined by 3D refined online server (Shuid *et al*., 2017). As a next approach after verifying the vaccine construct's structural integrity, we performed a stereochemical analysis, Z-score calculation, and Ramachandran plot using the PROCHECK v.3.5 server (Laskowski *et al*., 1993; Wiederstein & Sippl, 2007).

Vaccine constructs docking with TLR-2

The binding affinity of the vaccine construct with TLR-2 (PDB ID: 5D3I) was evaluated by molecular docking using the ClusPro 2.0 server. Both the TLR-2 receptor and the vaccine construct PDB files have been submitted to this server. The server finds the model with the lowest electrostatic energy by applying the Fourier correlation algorithm to the models. The most efficient vaccine-TLR-2 complex was chosen for further molecular dynamic simulation analysis based on its low binding energy (Kozakov *et al*., 2017).

Molecular dynamics simulations

The AMBER20 software package (Case *et al*., 2012) to run a 100ns MD simulation to refine and stabilize the docking generated vaccine-TLR2 complex following our previously defined protocol and parameters (Chohan *et al*., 2016; Rehman *et al*., 2019). The protein-protein complex was initially included in the Leap module to incorporate missing hydrogens, neutralize the system, solvate the complex, and generate parameter and coordinate files for the simulation system. After that, the system under investigation was submerged into a TIP3P (Jorgensen *et al*., 1983) water model's octahedron box at a minimum distance of 15 Å from the solute surface. Na+ salts were added to the vaccine-TLR-2 complex to keep the system neutral. Before beginning the MD simulation, the amount of energy was reduced in three stages to avoid steric clashes. The temperature rises gradually from 0 to 300 K in 100 picoseconds and remained at that level during an NVT ensemble. After that, an equilibration procedure was carried out on the vaccine-TLR2 complex by using the Langevin dynamics with a collision frequency of 1 PS-1 and maintaining a constant force of 10 kcal/(mol•1). In addition, an MD simulation including the NPT ensemble was carried out on the protein-protein complex while it was subjected to conditions of a pressure of 1 atm and a temperature of 300 K. To evaluate the electrostatic interactions, the particle-mesh-Ewald (PME) method was utilized (Darden *et al*., 1993). Trajectories from MD simulations were recorded at 1ps and 2ps for equilibration and production, respectively. AMBER 12 CARNAL, ANAL, and PTRAJ modules performed MD simulations.

To investigate dynamic stability and sampling pattern, MD analysis (MDa) was performed on the trajectories from the last 50ns of MD simulations, including 2D-RMSD, the radius of gyration (Rg), cross-correlation (DCCM) and principal component analysis (PCA) using the methodology developed by Arantes *et al*. (2021). MD analysis was performed for both the vaccine-bonded TLR2 complex and apo-TLR2 protein.

Free energy calculation. The MM/PB (GB) SA scoring method, which is based on molecular mechanics, was used to figure out the binding free energies of selected protein-protein complexes (Fogolari *et al*., 2003), performed in the amber20 software package. At first, a free vaccine construct (ligand) and a free TLR-2 (receptor) were put together to check that the complex was in equilibrium. The binding free energy was calculated as the difference between the combined free energies of the ligand-receptor complex (ΔGcom) and the sum of the free energies of the individual receptors (ΔGrec) and ligands (ΔGlig). To figure out the free energies of binding (ΔGbind), at least 4000 snapshots were taken every 5 ps from the last 20 ns of a steady MD trajectory.

Codon optimization and *In-silico* cloning

The proposed vaccine design undergoes a codon optimization method using the JCat (Java Codon adaption tool). An appropriate expression host was chosen to maximize the production of protein. The vaccine design was codon optimized in *Escherichia coli* (*E. coli*) strain K12 for protein expression. Codon adaptive index (CAI) value and GC content percentage are used to generate an output sequence of genes in JCat. A CAI of 0.8 or above is preferable, and whatever over 0.8 is acceptable, and a GC percentage of 30–70% is ideal. Finally, *XhoI* and *NdeI* restriction sites were added to the N- and C-terminal, respectively, of the codon-optimized sequence to clone it *In-silico* into the pET28(+) expression vector using the SnapGene software (Grote *et al*., 2005).

RESULTS

***Rhipicephalus microplus* selected proteins**

Three *R. microplus* proteins Bm86, Subolesin, and Bm95 amino acid sequences were retrieved from the NCBI dataset and analyzed using the scratch protein predictor; a score of >0.5 was deemed immunogenic. The precision of this approach exceeded 75%. All three proteins were antigenic, and their antigenic scores were more than 0.70 (Table 1).

Helper T-lymphocyte epitope identification

Prominent in triggering B-cell activation and cytotoxic T-cell responses to the foreign antigen, HTL epitopes also play a vital role in boosting the adaptive immune response. A total of 1426 (15-mer) HTL epitopes were predicted in this study using the IEDB-recommended 2.22 prediction methods. The selected epitopes all have IC50 values below 50nM and a percentile rank below 95. The binding affinity of an epitope increases as its percentile rank lowers. The top six most immunogenic epitopes out of 1,426 were selected based on their IC50 values of 10nM and their percentile ranks 5% (Khatoon *et al*., 2017). These six epitopes are further used for multi-epitopes-based vaccine construct (Table 2).

Identification of interferon-γ epitope

Epitopes associated with IFN-γ were predicted due to their role in boosting adaptive and innate immunological responses and activating MHC class II molecules. Induction of IFN- production by six of the HTL epitopes suggests their protective efficacy (Table 2).

Cytotoxic T-Lymphocyte epitope identification

Twenty-seven CTL epitopes were predicted from three *R. microplus* proteins by NetCTL 1.2 server. We chose three MHC class-I Supertypes A2, A3, and B7 for epitope prediction since they comprise 88.3% of the world's population. Specifically, CTL epitopes with scores of 0.75 or above were used in this study. Only 27 epitopes were identified with a score of 0.75 and only 8 CTL epitopes were shown to be highly immunogenic. Those were used in the designing of the vaccine (Table 3).

Prediction of B-cell epitope

The presentation of antigens triggers antibody production and the activation of memory B-cells via linear B-cell epitopes in the adaptive immune system. The ABCPred server was used to predict B-cell epitopes and the 11 highest-scoring B-cell epitopes were selected for use in vaccine designing (Table 4).

Table 1. *Rhipicephalus microplus* proteins predicted antigenic score

Sr. no.	Proteins	Accession no.	Predicted antigenic score
1.	Bm86	QOE77966	0.957
2.	Subolesin	AFQ91885	0.752
3.	Bm95	AAD38381	0.946

Table 2. Predicted HTL epitopes and IFN-γ inducer

Protein name	Selected Allele	Predicted Epitope	Percentile rank score	IC50 values	IFN-γ inducer	
					Result	Score
Bm86	HLA-DRB1*01:01	ATGLLLLLAATSVTA	0.01	1.00	Positive	0.49
		GLLLLLAATSVTAAS	0.01	2.00	Positive	0.50
Subolesin	HLA-DRB1*01:01	REEYDHVLSTKLAEQ	3.60	20.00	Positive	0.47
		EEYDHVLSTKLAEQY	4.50	21.00	Positive	0.47
Bm95	HLA-DRB1*01:01	GIALFVAAVSLIVEC	0.56	7.00	Positive	0.55
		MRGIALFVAAVSLIV	0.56	7.00	Positive	0.60

Table 3. Selected potential CTL epitopes of three proteins of *R. microplus*

Protein	Subertype A2		Subertype A3		Subertype B7	
	Predicted Epitope	Scoring	Selected Epitope	Scoring	Predicted Epitope	Scoring
Bm86	ALFVAAVSL	1.164	NMYFNAAEK	1.492	FAVMRGIAL	1.4926
	YTVSFTPNI	1.154	CTYERSTDK	1.404	NPSKGSTCV	1.016
	FVAAVSLIV	1.245	GITCKSISY	1.225	RNRGGTAKL	1.035
Subolesin	SPSGRSPKR	1.20	GLICERMMK	1.295	SPVHRDQPL	1.696
	SGRSPKRRR	1.17	RMMKERESK	1.211	SPKRRRCMP	0.948
	MPLSPPPTR	1.23	HSPSGRSPK	1.093	IAANIREEM	0.856
Bm95	FVAAVSLIV	1.244	NMYFNAAEK	1.492	HPIGEWCMM	1.180
	SIGKEVFKV	1.461	CLRPDLTCK	1.225	RPDLTCKDL	1.056
	YTVSFTPNI	1.155	LIAEKPLSK	1.397	FAVMRGIAL	1.035
	GIALFVAAV	1.143	PLSKYVLRK	1.206	CPSGSTVAE	1.040

Table 4. Predicted B-cell epitopes

Target protein	Epitope	Score (0.5)
Bm86	HEEFMDCGVYMNRQSC	0.95
	HGCTYERSTDKAYECT	0.95
	CYCPWKSRKPGPNVNI	0.94
Subolesin	TKLAEQYDTFVKFTYD	0.92
	RTHDWDPLHSPSGRSP	0.90
Bm95	HEEFMDCGVYMNRQSC	0.95
	ATTASTTTTKAKDKDP	0.93
	YCSPGSPKGPDGQCKN	0.92

Toxicity prediction

Toxinpred modules were used to determine the toxicity of epitopes, and it was found that six HTL, eight CTL, and eight B-cell epitopes were further used in the final vaccine design as they were found not toxic.

Design of a multi-epitope vaccine construct

Six helpers T-cell (HTL) epitopes, eight cytotoxic T-lymphocyte (CTL) epitopes, and eight B-cell epitopes with a score greater than 0.51 were chosen for use in the final vaccine design. The appropriate linker was used to connect these epitopes. The 50S ribosomal L7/L12 (P9WHE3) adjuvant was linked with HTL epitopes via the EAAAK linker to boost the vaccine's immunogenicity. We used the linkers AAY, KK, GPGPG, and EAAAK to make separate each epitope. Consequently, the full multiepitope vaccine design contains 490 amino acid residues, in addition to 1 EAAAK linker, 5 GPGPG linkers, 8 AAY linkers, and 8 KK linkers. The ultimate multi-epitope vaccine scheme is depicted concisely in Figure 1.

Evaluating immunogenicity, allergenicity, and physicochemical properties

The developed vaccine was immunogenic and antigenic, with VaxiJen v2.0 and ANTIGENpro predicting scores of 0.51 and 0.9351, respectively. In addition, the substance's allergenicity was evaluated so that inflammatory reactions might be prevented. AllerTOP v2.0 was used to evaluate the vaccine for allergenicity, and the results showed that it did not contain any allergenic components. The AlgPRED server was analyzed to measure that this vaccination has an allergenicity score of 0.420. The non-allergen threshold was kept at 0.4 throughout the process of this analysis. The physicochemical parameters revealed that the proposed vaccine had a total of 490 amino acids and a molecular weight of 53 kDa. With a theoretical pI value of 7.47 and an instability index of -40, the prediction indicated that the vaccine had a fundamentally stable and basic composition. The structure that was designed contained 61 amino acids with a positive charge and 60 with a negative charge. In yeast (*in vivo*), the half-life of the vaccine was >1 hour; in mammalian reticulocytes (*in vitro*), it was >30 hours; and in *E. coli*, it was >10 hours (*in vivo*). The hydrophobic character of the vaccine was shown by the fact that the suggested vaccine construct had an aliphatic index of 75.04 and a GRAVY score of -0.228. Antigenic, non-allergenic, thermostable, and hydrophobic were some of the defining characteristics of the vaccine that was developed.

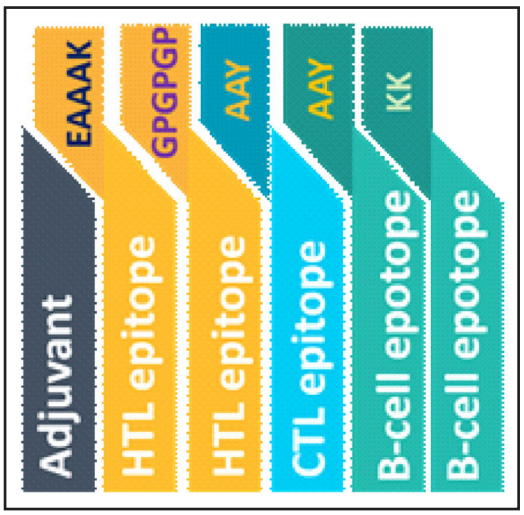

Figure 1. Schematic diagram of constructed multi-epitope vaccine. This vaccine is consisting of 490 amino acids residues, with 130 amino acids adjuvant followed by 6 HTL, 8 CTL and 8 B-cell epitopes. HTL epitopes has been linked with adjuvant by EAAAK linker. The GPGPG, AAY and KK linker were used to join HTL, CTL and B-cell epitopes respectively.

Prediction and validation of proposed vaccine secondary and tertiary structures

We analyzed the proposed vaccine's secondary structure and functional properties using the RaptorX server (Figure 2A). The projected secondary structure has a 5.3% B-sheet component, a 52.5% a-helix component, and a 40.2% coil component. The 3D structure was generated by RaptorX and passed through the PROCHECK server to build a Ramachandran plot (Figures 2B and C). According to the Ramachandran plot, 99.2% of the residues were placed in the favored region, 9.8% were found in the additional allowed region, 0.2% were situated in the generously allowed region, and 0% were located in the disallowed regions. In addition, the quality of the 3D model was evaluated with ERRAT by making use of the input structure. In the ERRAT study, the vaccine construct structure revealed a remarkable quality factor value of 98.0687, indicating that the built structure is of excellent quality. In addition, the 3D refined model was validated with the verify-3D tool (Figure 2C), which showed that 92.67% of residues have averaged 3D-1D scores that are more than 0.2, hence supporting the high-quality structure of the vaccine construct. The vaccine design was evaluated using the proSA web server to predict the z-score value. This value can indicate whether or not the structure is stable and suitable for docking analysis. If the z-value has a positive score, this indicates that the structure was not good, and a score that is equal to or more

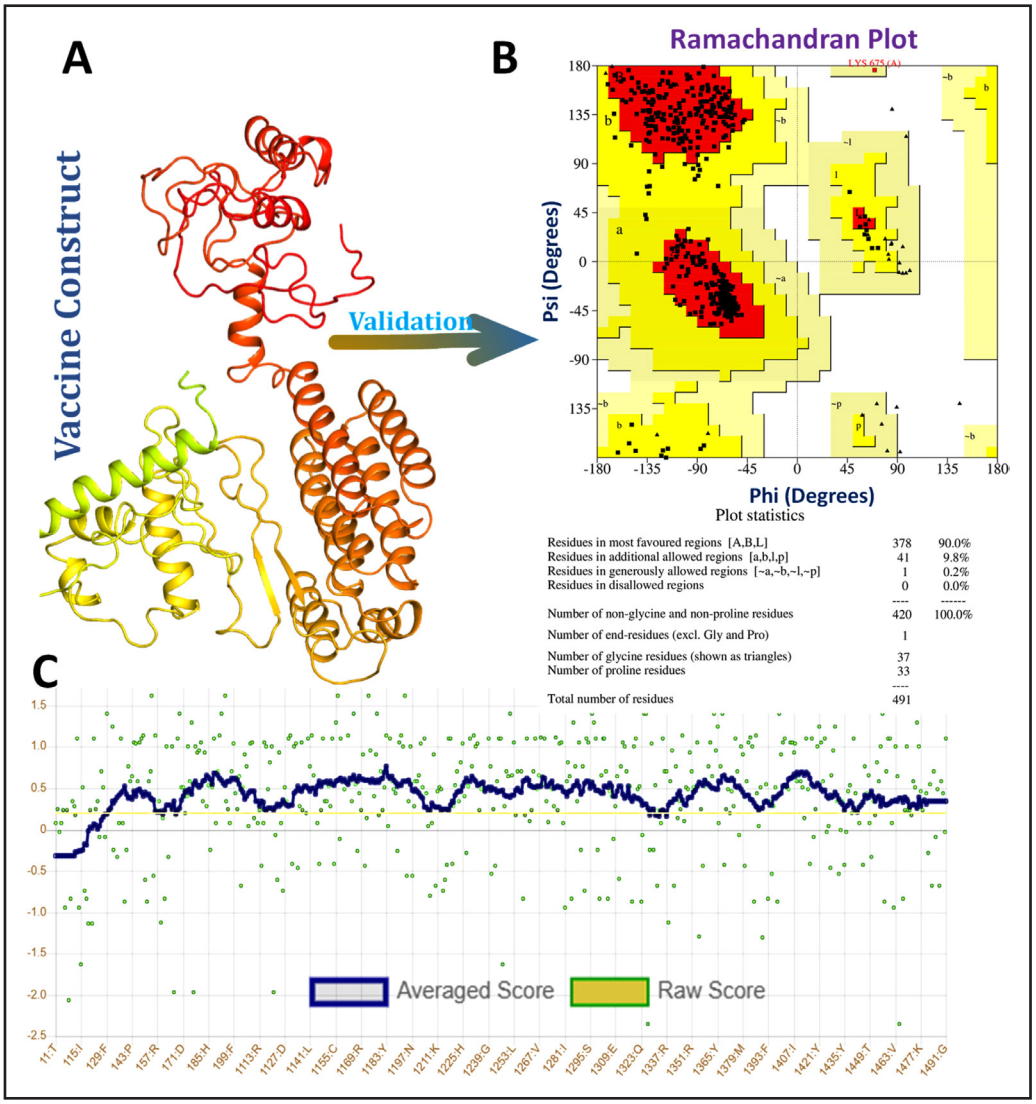

Figure 2. (A) Structures of vaccine construct built by RaptorX tool; (B) PROCHECK online webserver was used for Ramachandran plot analysis; (C) Plot generated by verifying 3D module of SAVES v6.0.

than -4 indicates an average structure. In our particular instance, the z-score fell within the range of (-8.93), which indicates that the developed vaccine construct falls inside the required Z-value range.

Molecular docking with TLR2

Ticks are arthropods that feed on blood and can be parasitic on vertebrates for a short period. Tick saliva contains biologically active molecules and suppressing the host immune response via the TLR2 pathway may benefit tick feeding and pathogen transmission (Kotál *et al*., 2015). TLR2 activation causes the recruit of adapter molecules e.g TIRAP, MyD88, IRAKs, and TRAF6, and activates the MAPK, IKK, and NF-B, as well as the up regulation of genes such as inducible nitric oxide synthase (iNOS), tumor necrosis factor-alpha (TNF-), and interleukin 6 (IL-6) (Keating *et al*., 2007). TLR2 agonists that have a higher binding affinity for TLR2 can induce both cellular and humoral immune responses as a result. Using the HADDOCK web server, an energy-optimized 3D model of the potential vaccine construct (Figure 3) was docked into TLR2 to assess whether or not the designed vaccine and the innate immune receptor interact with one another. A HADDOCK server divided the 188 potential structures into three separate clusters. These clusters together represent 94% of the models that were refined using water. The cluster with the greatest total score had a Z value of 1.2, and its total score was -72.3 +/- 4.7 kcal mol-1. According to the energy component analysis of HADDOCK scores, the principal driving forces for the creation of protein-protein complexes are electrostatic energies (GVdw= -111.7 kcal mol-1 and Gele= -360.1 kcal mol-1) and Van der Waals energies (Vdw= -360.1 kcal mol-1) respectively. The top-cluster models underwent one more round of refinement with the use of the HADDOCK refinement interface, which collated the twenty structures that stood out the most into a single cluster. This ultimate cluster consisted solely of water-refined models and has a HADDOCK score of -213.2 kcal mol-1. In addition, the final water-refined Model 1 was selected because it had the lowest docking energy score and the largest ligand RMSD. This allowed it to be used with the PRODIGY server to evaluate binding energy scores (Kd) (Xue *et al*., 2016). A lower Kd value indicates that two interacting proteins in a complex are stable and have a strong binding affinity. Vaccine-TLR2 exhibited weak stability and binding affinity at 25C° (ΔG=-11.4 kcal mol-1 and Kd (M) = 9.5 × 10-10), while the stability and binding affinity of protein-protein complex increases at optimal temperature (37 C°) ΔG=-12.3 kcal mol-1 and Kd (M) = 2.1 × 10-9, respectively. Overall the statistics obtained from HADDOCK and PRODIGY servers suggest that the vaccine construct is firmly intact with the TLR2 protein.

The top-ranked docking conformations for the protein-protein complex (Figure 3) were saved and graphically analyzed to uncover the crucial molecular connections underlying peptide-protein binding. As depicted in Figure 3A, the vaccine construct occupies the central domain of TLR2 to establish several H-bond, hydrophobic, and vdW contacts. In the vaccine-TLR2 complex, N296, F325, S329, S354, Q357, N379, Y376, E375, and K383 of key amino acids of TLR2 which may establish numerous H-bonds with adjacent residues of vaccine construct in the donor-acceptor motif (Figure 3B and C). The docking complex that was determined to be optimal for the vaccine-TLR2 system was then sent to the PDBsum web server so that a simplified 2D interaction diagram could be generated.

The PDBsum analysis (Figure 4) of the TLR2 bonded designed vaccine revealed nine H-bonds and one salt bridge. In addition, the vaccine construct contained 33 interface residues with a total area of 1403 Å2, whereas the corresponding TLR2 protein contained 25 interface residues with a total area of 1469 Å2. Moreover, the protein interaction analysis module of maestro illuminate was implicated to shed light on the molecular interaction of each residue individually. Figure 4 shows an example of residue mapping that is based on the pattern of interactions between proteins. This makes it simple to see how each residue contributes to the assembly of protein complexes.

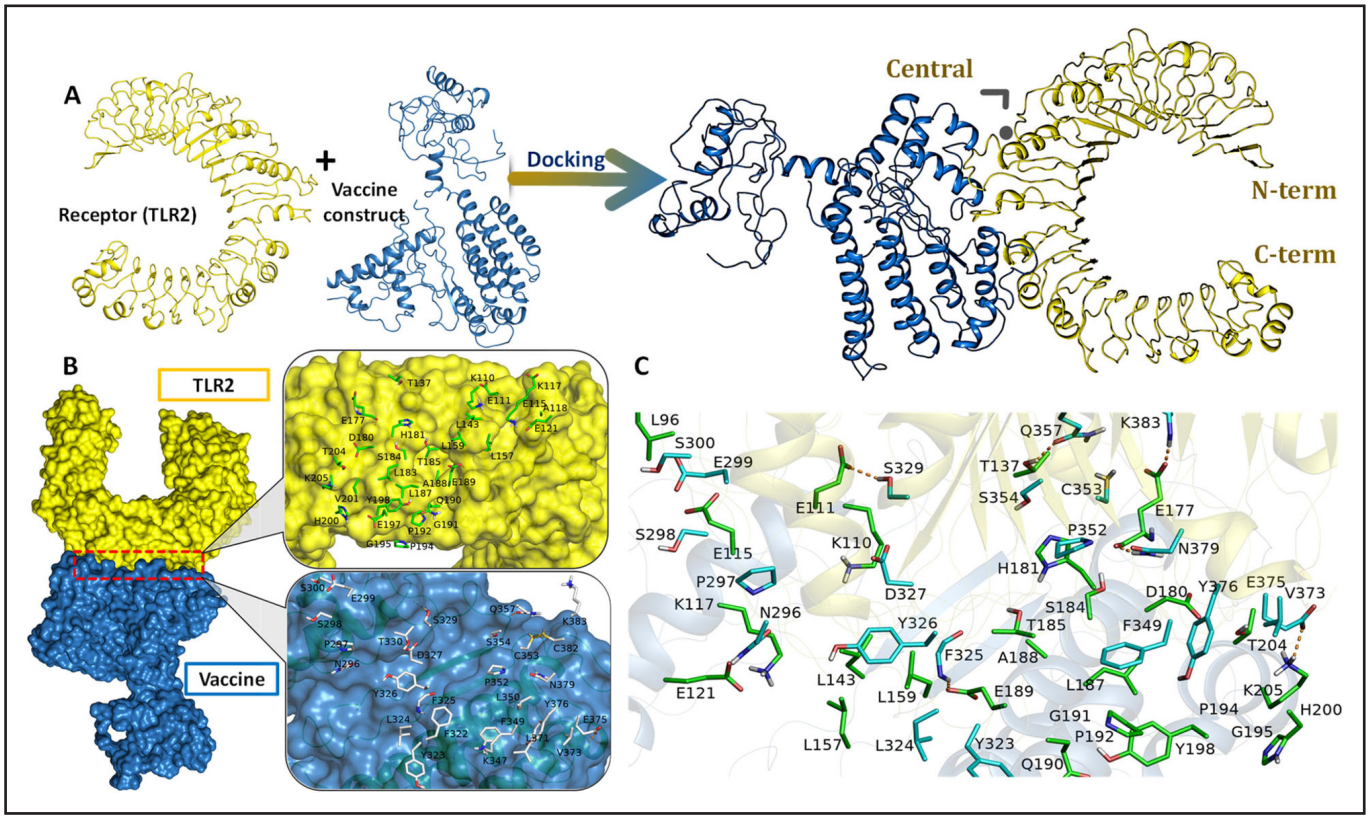

Figure 3. (A) Pre- and post-docking conformations of TLR2 (yellow) and Vaccine construct (blue); (B) Key amino acid of vaccine construct (green) interacting with TLR2 and Key amino acid of TLR2 (gray) interacting with vaccine construct; (C) Interaction between key amino acids in TLR2 (cyan) and their counterparts in the designed vaccine construct (green).

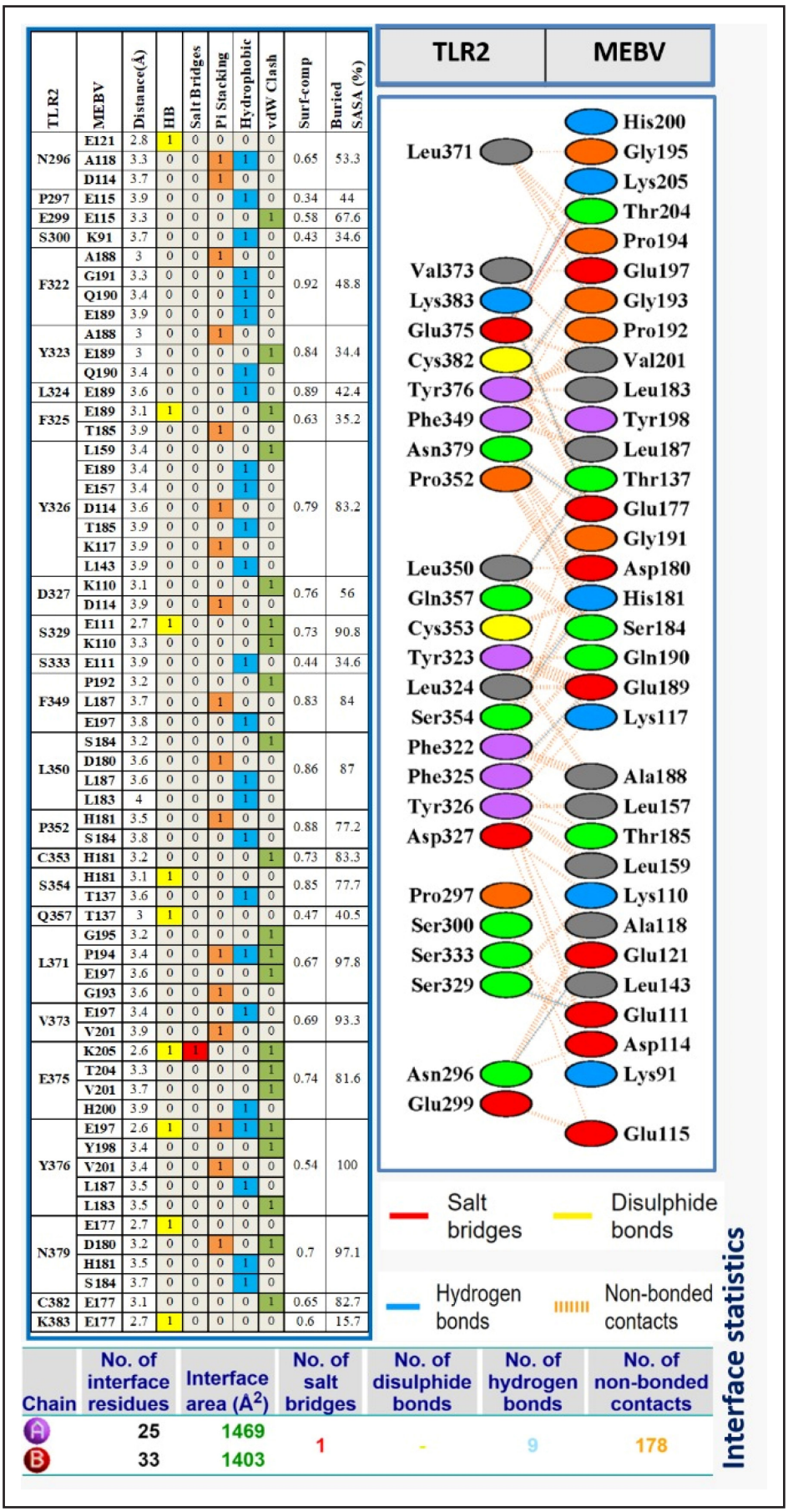

TLR2	MEBV	Distance(Å)	HB	Salt Bridges	PI Stacking	Hydrophobic	vdW Clash	Surf-comp	Buried SASA (%)
N296	E121	2.8	1	0	0	0	0	0.65	53.3
	A118	3.3	0	0	1	1	0		
	D114	3.7	0	0	1	0	0		
P297	E115	3.9	0	0	0	1	0	0.34	44
E299	E115	3.3	0	0	0	0	1	0.58	67.6
S300	K91	3.7	0	0	0	1	0	0.43	34.6
F322	A188	3	0	0	1	0	0	0.92	48.8
	G191	3.3	0	0	0	1	0		
	Q190	3.4	0	0	0	1	0		
	E189	3.9	0	0	0	1	0		
Y323	A188	3	0	0	1	0	0	0.84	34.4
	E189	3	0	0	0	0	1		
	Q190	3.4	0	0	0	1	0		
L324	E189	3.6	0	0	0	1	0	0.89	42.4
F325	E189	3.1	1	0	0	0	1	0.63	35.2
	T185	3.9	0	0	1	0	0		
Y326	L159	3.4	0	0	0	0	1	0.79	83.2
	E189	3.4	0	0	0	1	0		
	E157	3.4	0	0	0	1	0		
	D114	3.6	0	0	1	0	0		
	T185	3.9	0	0	0	1	0		
	K117	3.9	0	0	1	0	0		
	L143	3.9	0	0	0	1	0		
D327	K110	3.1	0	0	0	0	1	0.76	56
	D114	3.9	0	0	1	0	0		
S329	E111	2.7	1	0	0	0	1	0.73	90.8
	K110	3.3	0	0	0	0	1		
S333	E111	3.9	0	0	0	1	0	0.44	34.6
F349	P192	3.2	0	0	0	0	1	0.83	84
	L187	3.7	0	0	1	0	0		
	E197	3.8	0	0	0	1	0		
L350	S184	3.2	0	0	0	0	1	0.86	87
	D180	3.6	0	0	1	0	0		
	L187	3.6	0	0	0	1	0		
	L183	4	0	0	0	1	0		
P352	H181	3.5	0	0	1	0	0	0.88	77.2
	S184	3.8	0	0	0	1	0		
C353	H181	3.2	0	0	0	0	1	0.73	83.3
S354	H181	3.1	1	0	0	0	0	0.85	77.7
	T137	3.6	0	0	0	1	0		
Q357	T137	3	1	0	0	0	0	0.47	40.5
L371	G195	3.2	0	0	0	0	1	0.67	97.8
	P194	3.4	0	0	1	1	1		
	E197	3.6	0	0	0	0	1		
	G193	3.6	0	0	1	0	0		
V373	E197	3.4	0	0	0	1	0	0.69	93.3
	V201	3.9	0	0	1	0	0		
E375	K205	2.6	1	1	0	0	1	0.74	81.6
	T204	3.3	0	0	0	0	1		
	V201	3.7	0	0	0	0	1		
	H200	3.9	0	0	0	1	0		
Y376	E197	2.6	1	0	1	1	1	0.54	100
	Y198	3.4	0	0	0	0	1		
	V201	3.4	0	0	1	0	0		
	L187	3.5	0	0	0	1	0		
	L183	3.5	0	0	0	0	1		
N379	E177	2.7	1	0	0	0	0	0.7	97.1
	D180	3.2	0	0	1	0	1		
	H181	3.5	0	0	0	1	0		
	S184	3.7	0	0	0	1	0		
C382	E177	3.1	0	0	0	0	1	0.65	82.7
K383	E177	2.7	1	0	0	0	0	0.6	15.7

Interface statistics

Chain	No. of interface residues	Interface area (Å^2)	No. of salt bridges	No. of disulphide bonds	No. of hydrogen bonds	No. of non-bonded contacts
A	25	1469	1	-	9	178
B	33	1403				

Figure 4. Protein-Protein interaction fingerprinting represents the contribution of individual residue toward the vaccine-TLR2 complex formation. The presence and absence of residues are indicated by the numbers 1 and 0, respectively. The interactions between the residues are color-coded as hydrophobic (blue), H-bond (yellow), and salt-bridge (red). PDBsum generated a 2D-interaction diagram for interacting residues between docked vaccine construct and TLR2 protein.

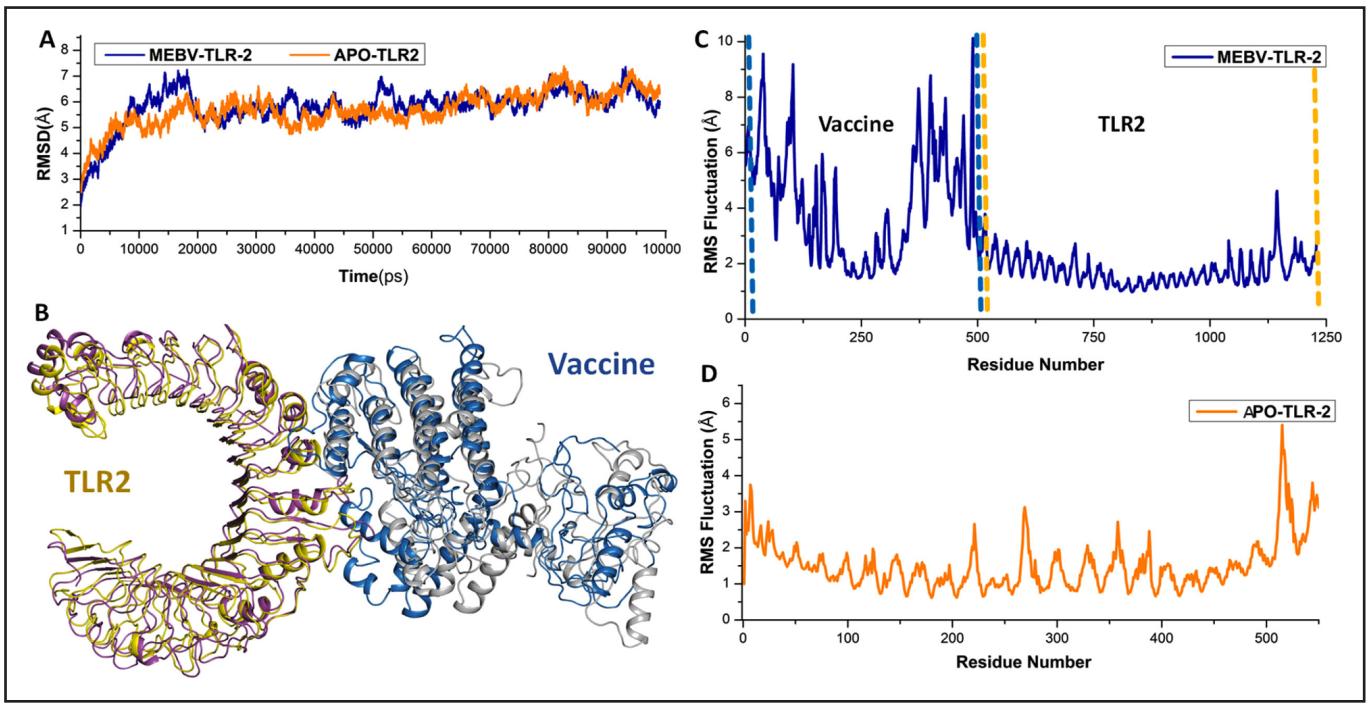

Figure 5. (A) RMSDs of Cα atoms of the vaccine-TLR2 complex backbone atoms of APO-TLR2 protein; (B) Structure comparison between initial (purple and blue) and representative snapshots from MD simulation (yellow and gray); (C) RMSF of each residue of the protein for the vaccine-TLR2 complex and; (D) APO-TLR2 protein obtained from 100 ns MD simulation.

Molecular dynamics simulations

Although molecular docking produces a suitable binding conformation, there are still several aspects that are not taken into account. The docking-generated conformation was then subjected to more accurate and robust MD simulations for 100 ns to gain insight into the binding mechanism, dynamic mobility, and stability of the vaccine-TLR2 complex in physiological settings. The binding free energies between the vaccine and the TLR-2 receptor were also calculated using the MM/PB(GB)SA technique. From its original conformation to its final state, the RMSD reveals how the protein's backbone has changed. To evaluate the dynamic stability of the vaccine-TLR-2 complex, the RMSD of the complex's backbone C atoms was computed over 100 ns of MD trajectories. Figure 5A showed the vaccine-TLR2 complex reached equilibrium within 15 ns after some initial fluctuation in the RMSD curve (1 to 3.2). The system stabilizes after equilibration, and it continued up to 100 ns. The RMSD of complexes varies after 15 ns by an average of 1.5, confirming. After every 15 ns, the RMSD of the complexes varied by an average of 1.5, confirming the stability of the vaccine-TLR2 system during MD simulation. Notably, the RMSD of apo-TLR2 protein follows a similar fluctuation pattern as that of the vaccine-TLR2 complex. These findings collectively imply that the TLR2 protein undergoes structural changes upon binding to the vaccine construct but remains firmly bonded to a vaccine. These conformational changes were verified by superimposing coordinates from a representative MD simulated snapshot onto the starting conformation (Figure 5B). The root-mean-square fluctuation (RMSF) vs the number of residues for the apo-TLR-2 protein and the vaccine-TLR-2 complex are displayed in Figures 5C and D, respectively. Toll-like receptor 2 (TLR2) protein structures, both in complex with a vaccine design and uncomplexed, exhibit a consistent RMSF pattern. A slightly greater RMSD value of the vaccination-TLR2 complex was observed when compared to the APO-TLR2 protein, which may be explained by the fact that the vaccine construct displayed larger variability of the residues in the vaccine-TLR2 system.

Table 5. Binding free energy of inhibitory compounds to TLR2

Complex	TLR2-vaccine
ΔE_{vdW}[a]	-70.12
ΔE_{ele}[a]	-41.69
$\Delta G_{nonpol, sol}$[a]	-8.03
ΔG_{gas}	-111.81
ΔG_{sol}	48.32
$\Delta G_{ele, sol (PB)}$[a]	71.08
$\Delta G_{ele, sol (GB)}$[a]	56.35
$\Delta E_{vdW}+\Delta G_{nonpol, sol}$[a]	-78.15
$\Delta E_{ele}+\Delta G_{ele, sol (PB)}$[a]	29.39
$\Delta E_{ele}+\Delta G_{ele, sol (GB)}$[a]	14.66
$\Delta G_{pred (PB)}$[b]	-37.13
$\Delta G_{pred (GB)}$[b]	-63.39

[a]All energies are in kcal/mol, ΔH: the enthalpy changes, ΔH = DG_{ele} + ΔG_{vdW} + $\Delta G_{nonpol, sol}$ + ΔGele, sol.
[b]ΔG_{pred}: the calculated binding free energy by the MMPB(GB)SA method.

Free energy calculation

Each vaccine-TLR2 system used 2000 snapshots from the final 10 ns of MD trajectories to calculate the binding free energies using MM/PBSA and MM/GBSA methods, providing a quantitative estimate of the binding strength of the vaccine-TLR2 complexes. Thermodynamic contributions and binding free energies for the TLR2-vaccine complex are summarized in Table 5. The projected binding free energy (ΔGpred (GB)) values of the TLR2-vaccine construct system (63.49 kcal·mol^{-1}) show that the vaccine is tightly bound to the TLR2 protein. Similarly, the vaccine design has a substantial affinity towards TLR2 as indicated by the Gpred (PB) values (37.13 kcal·mol^{-1}).

To further understand the elements that influence vaccines to construct binding to TLR2 protein, we used MMGB(PB)SA methods to dissect the overall binding free energies into their component binding free energy parts (Table 5). Computed values of individual binding free different components reveal that the unfavorable electrostatics of desolvation commitment is opposed to the favorable Coulomb interactions between the two proteins, suggesting that the total of the electrostatic interaction components in vacuum (ΔGele) and solvent (ΔGele, sol) is unfavorable to protein-protein binding. In contrast, an increase in both the vdW energy (ΔEvdW) and the nonpolar solubilization energy (ΔGnonpol, sol) is beneficial to the complex under study. In conclusion, ΔEvdW and ΔEele are essential for the vaccine construct to bind to TLR2.

***In silico* cloning and codon optimization**

Using *In silico* approach, for cloning of engineered vaccine in an appropriate expression vector, it is necessary to first codon optimizes the vaccine construct. CAI-value of 1.0 and GC content of 50% was achieved through codon optimization of the sequence. To facilitate cloning, the XhoI and NdeI restriction sites in the MCS of expression vector pET28a(+) were chosen. As can be seen in Figure 6, the length of the targeted gene was 1450 bp, whereas the restriction clone is 6763 bp in length.

DISCUSSION

Rhipicephalus microplus is a widely distributed tick in cattle and affects the health and production of cattle by reducing milk and meat production and transmitting various pathogens worldwide (Barker & Murrell, 2004; Peter *et al*., 2005). To control the tick infestations, the number of vaccine candidates has been identified (de la Fuente *et al*., 2007). However, due to *R. microplus* strain to-strain variation there is needed to develop a specific vaccine for better protection and control of cattle tick infestation. *Rhipicephalus microplus* antigens Bm86, Subolesin, and Bm95 can separately protect tick infestation (Dela Fuente *et al*., 2000; De Vos *et al*., 2001; Almazán *et al*., 2005; De la Fuente & Kocan, 2006). Using immune-informatics approaches, a multi-epitope-based vaccine was developed for ticks in this study, which suggests a promising direction for the future creation of an efficient antigenic vaccine. Since we only used an antigenic segment of the genome rather than the entire, the vaccine we developed in this study did not trigger any allergic reactions in the human subjects. In addition, the three *R. microplus* proteins included in our vaccine design all have MHC epitopes, HTL epitopes, and CTL epitopes, so it may be more effective than vaccines based on a single antigen. An adjuvant is used to boost the vaccine's immunogenicity in a vaccine design. Several studies have reported the advantages and experimental validation of multi-epitope vaccines using these immuno-informatic tools (Zheng *et al*., 2017; Kalita *et al*., 2020a). Several vaccines were developed by this method against various infectious diseases, and now have been experimentally validated and approved for clinical trials (Caro-Gomez *et al*., 2014; Mehla & Ramana, 2016; Jiang *et al*., 2017; Lu *et al*., 2017; He *et al*., 2018; Younas *et al*., 2023a).

Using a variety of immune epitope database tools, HTL, CTL, and B-cell epitopes of target *R. microplus* proteins were identified and characterized. Epitopes are the unique areas that are present on proteins and are important in the stimulation of immune responses at both the cellular and humoral levels (Mogensen, 2009). To reduce the likelihood of an autoimmune response occurring, we focused on identifying antigenic and non-allergenic regions within the *R. microplus* strain that were able to interact with a variety of HLA alleles (Bazhan *et al*., 2019). The vaccine was developed with the help of an adjuvant, as well as six HTL epitopes, eight CTL epitopes,

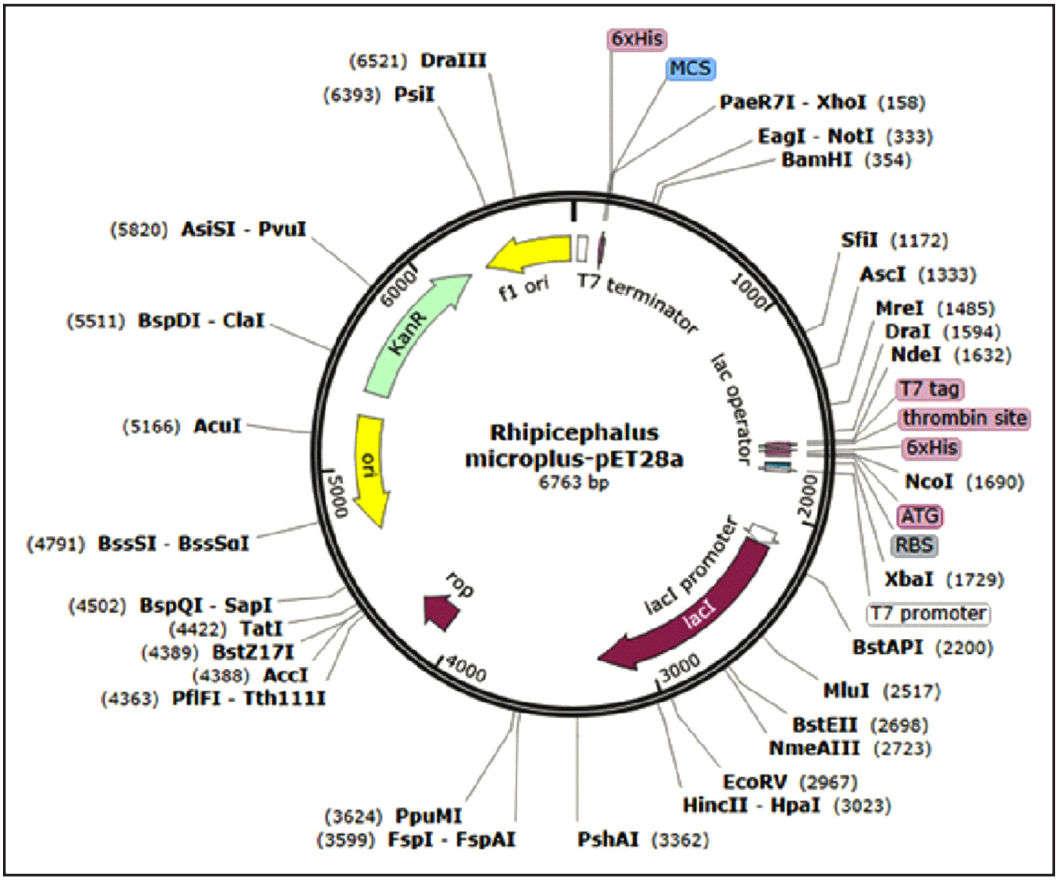

Figure 6. *In silico* cloning, a map shows how SnapGene software was used to add an optimized codon to the pET-28a (+) expression vector, which is unique to the design of the vaccine.

and eight B-cell epitopes (Table 2-4), all of which were linked to one another using GPGPG, AAY, and KK linkers, respectively (Narula *et al*., 2018). These linkers provide flexibility to the structure of proteins and caused immunogenicity in designed multi-epitope vaccines. GPGPG, AAY, and KK were included as linkers in previous literature to prevent the creation of junctional epitopes. In addition, Arai *et al*. (2001) found that the EAAAK linker had been included to combine the adjuvant with the remaining epitopes. This may have improved the stability and activity of the developed vaccine construct (Chen *et al*., 2013; Bazhan *et al*., 2019). To increase the efficacy of multi-epitope vaccines, the 50S ribosomal protein L7/L12 was employed as an adjuvant (Gupta *et al*., 2013). Ultimately, the length of the final vaccine designed was 490 amino acid residues, and a vaccine with these amino acids can be expressed and produced.

The vaccine that has been designed was evaluated and proven to be non-allergic and antigenic. It also has the potential to be employed. The physicochemical parameters revealed that the proposed vaccine had a total of 490 amino acids and a molecular weight of 53 kilodaltons. With a theoretical pI value of 7.47 and an instability index of -40, the prediction indicated that the vaccine had a fundamentally stable and basic composition. The structure that was created contained 61 amino acids with a positive charge and 60 with a negative charge. An aliphatic index of 75.04 was achieved by the vaccine construct that was created. Antigenic, non-allergenic, thermostable, and hydrophobic were some of the defining characteristics of the vaccine that was developed. The vaccine is hydrophilic, as demonstrated by a GRAVY value of -0.228; hence, it would interact with an environment that is predominately composed of water (Dodangeh *et al*., 2019). The shape of the protein structure is held together by the β-strand and α-helix, and the hydrogen bond energy in these structures shows that they interact with antibodies (Naveed *et al*., 2022). Then, the secondary structure of the constructed vaccine construct was analyzed by the RaptorX tool (Figure 2A), which assumed that the vaccine structure was made up of 5.3% β-strand, 52.5% α-helix, and 40.2% random coils. The higher percentage of β-strand and α-helix of the vaccine structure confirmed high hydrogen-bonding energy and retained the structure of the protein which assisted strong antibody interaction. The ERRAT, verify 3D and Ramachandran plots were used to assess the quality and reliability of the protein structures (Figures 2B and C). Ramachandran's plot showed that 99.2% of the residues were in the allowed area, 9.8% were in the additional allowed area, 0.2% was in the generously allowed area, and there were no residues in the not allowed area. ERRAT analysis showed that the vaccine construct structure has a high-quality factor value of 98.0687, which shows that the structure is of high quality. The 3D structure of the vaccine construct was also checked with the verify-3D tool (Figure 2C), which showed that 92.67% of residues have an average 3D-1D score of >0.2. This shows that the structure of vaccine construct 71 is of high quality. Also, the proSA online server looked at the vaccine construct to assess the Z-score value, which reveals if the structure is stable and ready for molecular docking analysis. The structure of our vaccine was good because the Z-score value was in the range of (-8.93).

In the present study, vaccine construct interaction and binding affinity with TLR2 were determined by the HADDOCK web server. As a result, TLR2 agonists with higher binding affinity for TLR2 may activate the innate and adaptive immune responses. Energy-optimized 3D models of the potential vaccine design were docked with TLR2 to assess for interaction (Figure 3). 94 % of the models that were improved with water were divided into three clusters by a HADDOCK server. One cluster had a Z value of 1.2 and an overall score of -72.3 +/- 4.7 kcal mol-1, making it the highest-scoring cluster. All the models in this last group had a HADDOCK score of -213.2 kcal mol, indicating that they had been refined using water. Also, the PRODIGY server was used to evaluate binding energy scores (Kd), and the final water-refined Model 1 was selected because it had the lowest docking energy score and the largest ligand RMSD (Xue *et al*., 2016). Overall, the numbers from the HADDOCK and PRODIGY servers show that the TLR2 protein in the vaccine is well-built and intact. Figure 3A shows that the vaccine construct is in the middle of TLR2 to make several H-bond, hydrophobic, and vdW contacts. In the vaccine-TLR2 complex, the key amino acids of TLR2 are N296, F325, S329, S354, Q357, N379, Y376, E375, and K383, which may make many H-bond contacts with the nearby residues of the vaccine construct. This is called a "donor-acceptor motif" (Figures 3B and C). The top-ranked vaccine-TLR2 docking complex was submitted to the PDBsum web server so that a simplified 2D interaction diagram could be made. The PDBsum analysis (Figure 4) of the TLR2 bonded designed vaccine revealed nine H-bonds and one salt bridge. In addition, the vaccine construct contained 33 interface residues with a total area of 1403 Å2, whereas the corresponding TLR2 protein contained 25 interface residues with a total area of 1469 Å2. To learn more about how the vaccine-TLR2 complex binds, and how it moves and stays stable in physiological conditions, the docking-generated structure was run through more accurate and robust MD simulations for 100 ns. The root-mean-square deviation (RMSD) shows how the backbone of a protein structure changes from its first shape to its final shape. Over 100 ns of MD trajectories, the change in the RMSD of the C atoms in the backbone of the vaccine-TLR-2 complex was calculated. This was done to check the dynamic stability of the studied complex system. Figure 5A showed that the vaccine-TLR2 complex reached equilibrium within 15 ns after some initial fluctuation in the RMSD curve (1 to 3.2). Figures 5C and D show the root-mean-square fluctuation (RMSF) for the apo-TLR-2 protein and the vaccine-TLR-2 complex as a function of the number of residues. But the residues in the vaccine-TLR2 system were more different in the vaccine construct, which may explain why the RMSD value of the vaccine-TLR2 complex was a little higher than that of the APO-TLR2 protein. MM/PBSA and MM/GBSA methods were used to calculate binding free energies for each vaccine-TLR2 system by taking 2000 snapshots from the last 10 ns of MD trajectories. This was done to measure how well the vaccine-TLR2 complexes stuck together. The values of the predicted binding free energy (Gpred (GB)) of the TLR2-vaccine construct system (63.49 kcal·mol^{-1}) show that the vaccine is strongly attached to the TLR2 protein. Also, the Gpred (PB) values for the vaccine-TLR2 system (37.13 kcal·mol^{-1}) show that there are strong interactions between the vaccine construct and TLR2. These results show that the designed vaccine construct-TLR-2 complex was less mobile and more stable in a state of atomism. However, the constructed vaccine that we have developed has the potential to stimulate both the humoral and cellular immune responses. It is antigenic, and non-allergenic and showed expression in *E. coli* (Figure 6). Immuno-informatic approaches help design multiepitope vaccines and reported by several studies (Ojha *et al*., 2019; Kar *et al*., 2020). In this study, we designed the vaccine construct using immuno-informatic approaches; however, it requires additional in vivo and *in vitro* evaluations to confirm the vaccination potential. These evaluations are currently being conducted in the laboratory, along with additional experiments.

CONCLUSION

Cattle farmers face a significant risk from tick-borne diseases like babesiosis and anaplasmosis, both of which are transmitted by the vector *R. microplus* tick. There is currently no reliable vaccination to guard against tick-borne diseases. Despite extensive research, no subunit recombinant vaccine has yet shown any significant promise. The goal of this research was to use a variety of immunoinformatics technologies to build a multi-epitope based vaccination against *R. microplus*. Our design construct for a multi-epitope based vaccination was verified as a promising vaccine candidate by molecular docking, molecular dynamic simulation, and *in-silico* cloning. These results pave the way for the development

of a vaccination against *R. microplus* ticks; nevertheless, additional experimental validation is required to prove the vaccine is safe and efficient in reducing tick populations.

ACKNOWLEDGEMENT

We thank the Molecular Parasitology Laboratory of Parasitology Department, UVAS, Lahore, Pakistan. This research was funded by HEC-GCF, grant number 273. This project is funded by Grand Challenges Funds of Higher Education Commission, Pakistan.

Conflict of interest

The authors declare no competing interests.

REFERENCES

Ahmad, T.A., Eweida, A.E. & Sheweita, S.A. (2016). B-cell epitope mapping for the design of vaccines and effective diagnostics. *Trials in Vaccinology* **5**: 71-83. https://doi.org/10.1016/j.trivac.2016.04.003

Almazán, C., Kocan, K.M., Blouin, E.F. & de la Fuente, J., (2005). Vaccination with recombinant tick antigens for the control of *Ixodes scapularis* adult infestations. *Vaccine* **23**: 5294-5298. https://doi.org/10.1016/j.vaccine.2005.08.004

Arai, R., Ueda, H., Kitayama, A., Kamiya, N. & Nagamune, T. (2001). Design of the linkers which effectively separate domains of a bifunctional fusion protein. *Protein engineering* **14**: 529-532. https://doi.org/10.1093/protein/14.8.529

Arantes, P.R., Polêto, M.D., Pedebos, C. & Ligabue-Braun, R. (2021). Making it rain: cloud-based molecular simulations for everyone. *Journal of Chemical Information and Modeling* **61**: 4852-4856. https://doi.org/10.1021/acs.jcim.1c00998

Barker, S.C. & Murrell, A., (2004). Systematics and evolution of ticks with a list of valid genus and species names. *Parasitology* **129**: S15-S36. https://doi.org/10.1017/S0031182004005207

Bazhan, S.I., Antonets, D.V., Karpenko, L.I., Oreshkova, S.F., Kaplina, O.N., Starostina, E.V., Dudko, S.G., Fedotova, S.A. & Ilyichev, A. (2019). In silico designed ebola virus t-cell multi-epitope DNA vaccine constructions are immunogenic in mice. *Vaccines* **7**: 34. https://doi.org/10.3390/vaccines7020034

Calis, J.J.A., Maybeno, M., Greenbaum, J.A., Weiskopf, D., De Silva, A.D., Sette, A., Keşmir, C. & Peters, B. (2013). Properties of MHC class I presented peptides that enhance immunogenicity. *PLoS Computational Biology* **9**: e1003266. https://doi.org/10.1371/journal.pcbi.1003266

Caro-Gomez, E., Gazi, M., Goez, Y. & Valbuena, G. (2014). Discovery of novel cross-protective *Rickettsia prowazekii* T-cell antigens using a combined reverse vaccinology and *in vivo* screening approach. *Vaccine* **32**: 4968-4976. https://doi.org/10.1016/j.vaccine.2014.06.089

Case, D.A., Darden, T.A., Cheatham III, T.E., Simmerling, C.L., Wang, J., Duke, R.E., Luo, R., Walker, R.C., Zhang, W., Merz, K.M. *et al*. (2012). AMBER 12. University of California, San Francisco.

Chen, X., Zaro, J.L. & Shen, W.C. (2013). Fusion protein linkers: property, design and functionality. *Advanced Drug Delivery Reviews* **65**: 1357-1369. https://doi.org/10.1016/j.addr.2012.09.039

Childs, M.L., Baskerville, E.B. & Cobey, S. (2015). Trade-offs in antibody repertoires to complex antigens. *Philosophical Transactions of the Royal Society B: Biological Sciences* **370**: 20140245. https://doi.org/10.1098/rstb.2014.0245

Chohan, T.A., Qian, H., Pan, Y. & Chen, J. (2016). Molecular simulation studies on the binding selectivity of 2-anilino-4-(thiazol-5-yl)-pyrimidines in complexes with CDK2 and CDK7. *Molecular BioSystems* **12**: 145-161. https://doi.org/10.1039/C5MB00630A

Darden, T., York, D. & Pedersen, L. (1993). Particle mesh Ewald: an *N*-log(*N*) method for Ewald sums in large systems. *The Journal of Chemical Physics* **98**: 10089-10092. https://doi.org/10.1063/1.464397

de la Fuente, J., Almazán, C., Canales, M., de la Lastra, J.M.P., Kocan, K.M. & Willadsen, P. (2007). A ten-year review of commercial vaccine performance for control of tick infestations on cattle. *Animal Health Research Reviews* **8**: 23-28. https://doi.org/10.1017/S1466252307001193

De la Fuente, J. & Kocan, K. (2006). Strategies for development of vaccines for control of ixodid tick species. *Parasite Immunology* **28**: 275-283. https://doi.org/10.1111/j.1365-3024.2006.00828.x

De La Fuente, J., Rodríguez, M., Redondo, M., Montero, C., García-García, J., Méndez, L., Serrano, E., Valdés, M., Enriquez, A., Canales, M. *et al*. (1998). Field studies and cost-effectiveness analysis of vaccination with Gavac™ against the cattle tick *Boophilus microplus*. *Vaccine* **16**: 366-373. https://doi.org/10.1016/S0264-410X(97)00208-9

De Vos, S., Zeinstra, L., Taoufik, A., Willadsen, P. & Jongejan, F. (2001). Evidence for the utility of the Bm86 antigen from *Boophilus microplus* in vaccination against other tick species. *Experimental & Applied Acarology* **25**: 245-261. https://doi.org/10.1023/A:1010609007009

Dela Fuente, J., Rodriguez, M. & García-García, J.C. (2000). Immunological control of ticks through vaccination with *Boophilus microplus* gut antigens. *Annals of the New York Academy of Sciences* **916**: 617-621. https://doi.org/10.1111/j.1749-6632.2000.tb05347.x

Dhanda, S.K., Vir, P. & Raghava, G.P.S. (2013). Designing of interferon-gamma inducing MHC class-II binders. *Biology Direct* **8**: 30. https://doi.org/10.1186/1745-6150-8-30

Dimitrov, I., Bangov, I., Flower, D.R. & Doytchinova, I. (2014). Allertop v. 2 – a server for *in silico* prediction of allergens. *Journal of Molecular Modeling* **20**: 2278. https://doi.org/10.1007/s00894-014-2278-5

Dodangeh, S., Daryani, A., Sharif, M., Aghayan, S.A., Pagheh, A.S., Sarvi, S. & Rezaei, F. (2019). A systematic review on efficiency of microneme proteins to induce protective immunity against *Toxoplasma gondii*. *European Journal of Clinical Microbiology & Infectious Diseases* **38**: 617-629. https://doi.org/10.1007/s10096-018-03442-6

Doytchinova, I.A. & Flower, D.R. (2007). VaxiJen: a server for prediction of protective antigens, tumour antigens and subunit vaccines. *BMC Bioinformatics* **8**: 4. https://doi.org/10.1186/1471-2105-8-4

Estrada-Peña, A., Bouattour, A., Camicas, J.-L., Guglielmone, A., Horak, I., Jongejan, F., Latif, A., Pegram, R. & Walker, A. (2006). The known distribution and ecological preferences of the tick subgenus *Boophilus* (Acari: Ixodidae) in Africa and Latin America. *Experimental & Applied Acarology* **38**: 219-235. https://doi.org/10.1007/s10493-006-0003-5

Fogolari, F., Brigo, A. & Molinari, H. (2003). Protocol for MM/PBSA molecular dynamics simulations of proteins. *Biophysical Journal* **85**: 159-166. https://doi.org/0006-3495/03/07/159/08

Fragoso, H., Rad, P.H., Ortiz, M., Rodriguez, M., Redondo, M., Herrera, L. & de la Fuente, J. (1998). Protection against *Boophilus annulatus* infestations in cattle vaccinated with the *B. microplus* Bm86-containing vaccine Gavac. *Vaccine* **16**: 1990-1992. https://doi.org/10.1016/S0264-410X(98)00116-9

Freeman, J.M., Davey, R.B., Kappmeyer, L.S., Kammlah, D.M. & Olafson, P.U. (2010). Bm86 midgut protein sequence variation in South Texas cattle fever ticks. *Parasites & Vectors* **3**: 101. https://doi.org/10.1186/1756-3305-3-101

Gaafar, B.B.M., Ali, S.A., Abd-Elrahman, K.A. & Almofti, Y.A., (2019). Immunoinformatics approach for multiepitope vaccine prediction from H, M, F, and N proteins of Peste des Petits ruminants virus. *Journal of Immunology Research* **2019**: 6124030. https://doi.org/10.1155/2019/6124030

García-García, J.C., Gonzalez, I.L., González, D.M., Valdés, M., Méndez, L., Lamberti, J., D'Agostino, B., Citroni, D., Fragoso, H., Ortiz, M. *et al*. (1999). Sequence variations in the *Boophilus microplus* Bm86 locus and implications for immunoprotection in cattle vaccinated with this antigen. *Experimental & Applied Acarology* **23**: 883-895. https://doi.org/10.1023/A:1006270615158

Gasteiger, E., Hoogland, C., Gattiker, A., Duvaud, S., Wilkins, M.R., Appel, R.D. & Bairoch, A. (2005). Protein identification and analysis tools on the ExPASy server. In: The Proteomics Protocols Handbook, Walker, J.M. (editor). Totowa: Humana Press, pp. 571-607. https://doi.org/10.1385/1-59259-890-0:571

Gershoni, J.M., Roitburd-Berman, A., Siman-Tov, D.D., Freund, N.T. & Weiss, Y. (2007). Epitope mapping. *BioDrugs* **21**: 145-156. https://doi.org/10.2165/00063030-200721030-00002

Graf, J.-F., Gogolewski, R., Leach-Bing, N., Sabatini, G.A., Molento, M.B., Bordin, E.L. & Arantes, G.J. (2004). Tick control: an industry point of view. *Parasitology* **129**: S427-S442. https://doi.org/10.1017/S0031182004006079

Grote, A., Hiller, K., Scheer, M., Münch, R., Nörtemann, B., Hempel, D.C. & Jahn, D. (2005). JCat: a novel tool to adapt codon usage of a target gene to its potential expression host. *Nucleic Acids Research* **33**: W526-W531. https://doi.org/10.1093/nar/gki376

Gupta, S., Kapoor, P., Chaudhary, K., Gautam, A., Kumar, R., Consortium, O.S.D.D. & Raghava, G.P.S. (2013). *In silico* approach for predicting toxicity of peptides and proteins. *PLOS ONE* **8**: e73957. https://doi.org/10.1371/journal.pone.0073957

He, R., Yang, X., Liu, C., Chen, X., Wang, L., Xiao, M., Ye, J., Wu, Y. & Ye, L. (2018). Efficient control of chronic LCMV infection by a CD4 T cell epitope-based heterologous prime-boost vaccination in a murine model. *Cellular & Molecular Immunology* **15**: 815-826. https://doi.org/10.1038/cmi.2017.3

Jiang, P., Cai, Y., Chen, J., Ye, X., Mao, S., Zhu, S., Xue, X., Chen, S. & Zhang, L. (2017). Evaluation of tandem *Chlamydia trachomatis* MOMP multi-epitopes vaccine in BALB/c mice model. *Vaccine* **35**: 3096-3103. https://doi.org/10.1016/j.vaccine.2017.04.031

Jorgensen, W.L., Chandrasekhar, J., Madura, J.D., Impey, R.W. & Klein, M.L. (1983). Comparison of simple potential functions for simulating liquid water. The *Journal of Chemical Physics* **79**: 926-935. https://doi.org/10.1063/1.445869

Kalita, J., Padhi, A.K. & Tripathi, T. (2020a). Designing a vaccine for fascioliasis using immunogenic 24 kda mu-class glutathione s-transferase. *Infection, Genetics and Evolution* **83**: 104352. https://doi.org/10.1016/j.meegid.2020.104352

Kalita, P., Padhi, A.K., Zhang, K.Y.J. & Tripathi, T. (2020b). Design of a peptide-based subunit vaccine against novel coronavirus SARS-CoV-2. *Microbial Pathogenesis* **145**: 104236. https://doi.org/10.1016/j.micpath.2020.104236

Källberg, M., Margaryan, G., Wang, S., Ma, J. & Xu, J. (2014). RaptorX server: a resource for template-based protein structure modeling. In: Protein Structure Prediction: Methods in Molecular Biology, vol 1137, Kihara, D. (editor). New York: Humana Press, pp. 17-27. https://doi.org/10.1007/978-1-4939-0366-5_2

Kar, T., Narsaria, U., Basak, S., Deb, D., Castiglione, F., Mueller, D.M. & Srivastava, A.P. (2020). A candidate multi-epitope vaccine against SARS-CoV-2. *Scientific Reports* **10**: 10895. https://doi.org/10.1038/s41598-020-67749-1

Keating, S.E., Maloney, G.M., Moran, E.M. & Bowie, A.G. (2007). IRAK-2 participates in multiple toll-like receptor signaling pathways to NFκB via activation of TRAF6 ubiquitination. *Journal of Biological Chemistry* **282**: 33435-33443. https://doi.org/10.1074/jbc.M705266200

Khatoon, N., Pandey, R.K. & Prajapati, V.K. (2017). Exploring *Leishmania* secretory proteins to design B and T cell multi-epitope subunit vaccine using immunoinformatics approach. *Scientific Reports* **7**: 8285. https://doi.org/10.1038/s41598-017-08842-w

Kotál, J., Langhansová, H., Lieskovská, J., Andersen, J.F., Francischetti, I.M., Chavakis, T., Kopecký, J., Pedra, J.H., Kotsyfakis, M. & Chmelař, J. (2015). Modulation of host immunity by tick saliva. *Journal of Proteomics* **128**: 58-68. https://doi.org/10.1016/j.jprot.2015.07.005

Kozakov, D., Hall, D.R., Xia, B., Porter, K.A., Padhorny, D., Yueh, C., Beglov, D. & Vajda, S. (2017). The ClusPro web server for protein–protein docking. *Nature Protocols* **12**: 255-278. https://doi.org/10.1038/nprot.2016.169

Larsen, M.V., Lundegaard, C., Lamberth, K., Buus, S., Lund, O. & Nielsen, M. (2007). Large-scale validation of methods for cytotoxic T-lymphocyte epitope prediction. *BMC Bioinformatics* **8**: 424. https://doi.org/10.1186/1471-2105-8-424

Laskowski, R.A., MacArthur, M.W., Moss, D.S. & Thornton, J.M. (1993). PROCHECK: A program to check the stereochemical quality of protein structures. *Journal of Applied Crystallography* **26**: 283-291. https://doi.org/10.1107/S0021889892009944

Lin, H.H., Zhang, G.L., Tongchusak, S., Reinherz, E.L. & Brusic, V. (2008). Evaluation of MHC-II peptide binding prediction servers: applications for vaccine research. *BMC Bioinformatics* **9**: 1-10. https://doi.org/10.1186/1471-2105-9-S12-S22

Lu, I.-N., Farinelle, S., Sausy, A. & Muller, C.P. (2017). Identification of a CD4 T-cell epitope in the hemagglutinin stalk domain of pandemic H1N1 influenza virus and its antigen-driven TCR usage signature in BALB/c mice. *Cellular & Molecular Immunology* **14**: 511-520. https://doi.org/10.1038/cmi.2016.20

Magnan, C.N., Zeller, M., Kayala, M.A., Vigil, A., Randall, A., Felgner, P.L. & Baldi, P. (2010). High-throughput prediction of protein antigenicity using protein microarray data. *Bioinformatics* **26**: 2936-2943. https://doi.org/10.1093/bioinformatics/btq551

Malik, A.A., Ojha, S.C., Schaduangrat, N. & Nantasenamat, C. (2022). ABCpred: a webserver for the discovery of acetyl-and butyryl-cholinesterase inhibitors. *Molecular Diversity* **26**: 467-487. https://doi.org/10.1007/s11030-021-10292-6

Marciani, D.J. (2003). Vaccine adjuvants: role and mechanisms of action in vaccine immunogenicity. *Drug Discovery Today* **8**: 934-943. https://doi.org/10.1016/S1359-6446(03)02864-2

McGuffin, L.J., Bryson, K. & Jones, D.T. (2000). The PSIPRED protein structure prediction server. *Bioinformatics* **16**: 404-405. https://doi.org/10.1093/bioinformatics/16.4.404

Mehla, K. & Ramana, J. (2016). Identification of epitope-based peptide vaccine candidates against enterotoxigenic *Escherichia coli*: a comparative genomics and immunoinformatics approach. *Molecular BioSystems* **12**: 890-901. https://doi.org/10.1039/C5MB00745C

Mogensen, T.H. (2009). Pathogen recognition and inflammatory signaling in innate immune defenses. *Clinical Microbiology Reviews* **22**: 240-273. https://doi.org/10.1128/cmr.00046-08

Narula, A., Pandey, R.K., Khatoon, N., Mishra, A. & Prajapati, V.K. (2018). Excavating chikungunya genome to design B and T cell multi-epitope subunit vaccine using comprehensive immunoinformatics approach to control chikungunya infection. *Infection, Genetics and Evolution* **61**: 4-15. https://doi.org/10.1016/j.meegid.2018.03.007

Naveed, M., Yaseen, A.R., Khalid, H., Ali, U., Rabaan, A.A., Garout, M., Halwani, M.A., Al Mutair, A., Alhumaid, S., Al Alawi, Z. *et al*. (2022). Execution and design of an anti HPIV-1 vaccine with multiple epitopes triggering innate and adaptive immune responses: an immunoinformatic approach. *Vaccines* **10**: 869. https://doi.org/10.3390/vaccines10060869

Ojha, R., Pareek, A., Pandey, R.K., Prusty, D. & Prajapati, V.K. (2019). Strategic development of a next-generation multi-epitope vaccine to prevent Nipah virus zoonotic infection. *ACS Omega* **4**: 13069-13079. https://doi.org/10.1021/acsomega.9b00944

Pandey, R.K., Ali, M., Ojha, R., Bhatt, T.K. & Prajapati, V.K. (2018). Development of multi-epitope driven subunit vaccine in secretory and membrane protein of *Plasmodium falciparum* to convey protection against malaria infection. *Vaccine* **36**: 4555-4565. https://doi.org/10.1016/j.vaccine.2018.05.082

Patarroyo, J.H., Portela, R.W., De Castro, R.O., Pimentel, J.C., Guzman, F., Patarroyo, M.E., Vargas, M.I., Prates, A.A. & Mendes, M.A.D. (2002). Immunization of cattle with synthetic peptides derived from the *Boophilus microplus* gut protein (Bm86). *Veterinary Immunology and Immunopathology* **88**: 163-172. https://doi.org/10.1016/S0165-2427(02)00154-X

Peter, R.J., Van den Bossche, P., Penzhorn, B.L. & Sharp, B. (2005). Tick, fly, and mosquito control – lessons from the past, solutions for the future. *Veterinary Parasitology* **132**: 205-215. https://doi.org/10.1016/j.vetpar.2005.07.004

Rand, K.N., Moore, T., Sriskantha, A., Spring, K., Tellam, R., Willadsen, P. & Cobon, G.S. (1989). Cloning and expression of a protective antigen from the cattle tick *Boophilus microplus*. *Proceedings of the National Academy of Sciences* **86**: 9657-9661. https://doi.org/10.1073/pnas.86.24.9657

Rehman, K., Chohan, T.A., Waheed, I., Gilani, Z. & Akash, M.S.H. (2019). Taxifolin prevents postprandial hyperglycemia by regulating the activity of α-amylase: evidence from an *in vivo* and *in silico* studies. *Journal of Cellular Biochemistry* **120**: 425-438. https://doi.org/10.1002/jcb.27398

Rodríguez, M., Rubiera, R., Penichet, M., Montesinos, R., Cremata, J., Falcón, V., Sánchez, G., Bringas, R., Cordovés, C., Valdés, M. *et al*. (1994). High level expression of the *B. microplus* Bm86 antigen in the yeast *Pichia pastoris* forming highly immunogenic particles for cattle. *Journal of Biotechnology* **33**: 135-146. https://doi.org/10.1016/0168-1656(94)90106-6

Shaffer, J.S., Moore, P.L., Kardar, M. & Chakraborty, A.K. (2016). Optimal immunization cocktails can promote induction of broadly neutralizing Abs against highly mutable pathogens. *Proceedings of the National Academy of Sciences* **113**: E7039-E7048. https://doi.org/10.1073/pnas.1614940113

Shuid, A.N., Kempster, R. & McGuffin, L.J. (2017). ReFOLD: a server for the refinement of 3D protein models guided by accurate quality estimates. *Nucleic Acids Research* **45**: W422-W428. https://doi.org/10.1093/nar/gkx249

Sonenshine, D.E., Kocan, K.M. & de la Fuente, J. (2006). Tick control: further thoughts on a research agenda. *Trends in Parasitology* **22**: 550-551. https://doi.org/10.1016/j.pt.2006.09.003

Valle, M.R., Mèndez, L., Valdez, M., Redondo, M., Espinosa, C.M., Vargas, M., Cruz, R.L., Barrios, H.P., Seoane, G., Ramirez, E.S. *et al*. (2004). Integrated control of *Boophilus microplus* ticks in Cuba based on vaccination with the anti-tick vaccine Gavac™. *Experimental & Applied Acarology* **34**: 375-382 https:// doi.org/10.1007/s10493-004-1389-6

Wiederstein, M. & Sippl, M.J. (2007). ProSa-web: interactive web service for the recognition of errors in three-dimensional structures of proteins. *Nucleic Acids Research* **35**: W407-W410. https://doi.org/10.1093/nar/gkm290

Willadsen, P. (2006). Tick control: thoughts on a research agenda. *Veterinary Parasitology* **138**: 161-168. https://doi.org/10.1016/j.vetpar.2006.01.050

Willadsen, P., Riding, G.A., McKenna, R.V., Kemp, D.H., Tellam, R.L., Nielsen, J.N., Lahnstein, J., Cobon, G.S. & Gough, J.M. (1989). Immunologic control of a parasitic arthropod. Identification of a protective antigen from *Boophilus microplus*. *The Journal of Immunology* **143**: 1346-1351 https://doi.org/10.4049/jimmunol.143.4.1346

Xue, L.C., Rodrigues, J.P., Kastritis, P.L., Bonvin, A.M. & Vangone, A. (2016). PRODIGY: a web server for predicting the binding affinity of protein–protein complexes. *Bioinformatics* **32**: 3676-3678. https://doi.org/10.1093/bioinformatics/btw514

Yadav, S., Prakash, J., Shukla, H., Das, K.C., Tripathi, T. & Dubey, V.K. (2020). Design of a multi-epitope subunit vaccine for immune-protection against Leishmania parasite. *Pathogens and Global Health* **114**: 471-481. https://doi.org/10.1080/20477724.2020.1842976

Younas, M., Ashraf, K., Rashid, M.I., Ijaz, M., Suleman, M., Chohan, T.A. & Sarfraz-ur-Rahman. (2023a). Expression and purification of recombinant multi-epitope protein of *Rhipicephalus microplus* tick and its antigenicity in the rabbits model. *Pakistan Veterinary Journal* **43**: 778-784. http://doi.org/10.29261/pakvetj/2023.086

Younas, M., Rehman, R.M., Hussain, N., Shabir, S., Abbasi, A.M., Rahman, Z.U., Nasir, S., Khalid, A., Karim, J. & Khalid, A.R. (2023b). First report of *Neospora caninum*-associated aborted calve brain tissue in Punjab, Pakistan. *Veterinary Sciences and One Health Journal* **2**: 1-6.

Zhang, L. (2018). Multi-epitope vaccines: a promising strategy against tumors and viral infections. *Cellular & Molecular Immunology* **15**: 182-184. https://doi.org/10.1038/cmi.2017.92

Zheng, J., Lin, X., Wang, X., Zheng, L., Lan, S., Jin, S., Ou, Z. & Wu, J. (2017). In silico analysis of epitope-based vaccine candidates against Hepatitis B virus polymerase protein. *Viruses* **9**: 112. https://doi.org/10.3390/v9050112